

Magnetic transition in highly frustrated $\text{SrCr}_8\text{Ga}_4\text{O}_{19}$: The archetypal *kagomé* system

B. Martínez

*Instituto de Ciencia de Materiales de Barcelona, Consejo Superior de Investigaciones Científicas,
Campus Universidad Autónoma de Barcelona, Bellaterra 08193, Spain*

A. Labarta

Departamento de Física Fundamental, Universidad de Barcelona, Diagonal 647, Barcelona 08028, Spain

R. Rodríguez-Solá

Escola Técnica de Vilanova, U.P.C., Vilanova i Geltru, Spain

X. Obradors

*Instituto de Ciencia de Materiales de Barcelona, Consejo Superior de Investigaciones Científicas,
Campus Universidad Autónoma de Barcelona, Bellaterra 08193, Spain*

(Received 21 January 1994; revised manuscript received 4 April 1994)

Both dc and ac magnetic susceptibility have been carefully measured and analyzed in order to determine the features of the low-temperature magnetic state of the highly frustrated $\text{SrCr}_8\text{Ga}_4\text{O}_{19}$ compound. The scaling analysis of the nonlinear part of the dc magnetic susceptibility gives clues that indicate that the nature of the magnetic state below T_f does not correspond to a conventional spin glass. This idea is further confirmed by the study of the dynamic scaling that also differs from what is expected for a conventional spin glass. A progressive change towards a more conventional magnetic ordering below T_f is observed by substituting Ga atoms by Fe atoms in the compound $\text{SrCr}_8\text{Ga}_{4-2x}\text{Fe}_x\text{O}_{19}$. For $x = 1.5$, both the scaling analysis of the nonlinear part of the dc magnetic susceptibility and the dynamic scaling seem to indicate that a true spin-glass phase transition does exist at T_f . This change in the magnetic behavior is attributed to the fact that the presence of a magnetic atom in the $4f_{VI}$ sites as a first neighbor of the Cr atoms, located in the 12k sites, will impose a "local preferential direction" for the magnetic moments removing somehow the strong intrinsic magnetic frustration of the *kagomé* lattice.

INTRODUCTION

Antiferromagnetic interactions between magnetic moments arranged in geometrical units that frustrate the formation of ordered states usually leads to magnetic system that exhibit a highly degenerated ground state, which may be magnetically disordered^{1,2} or unconventional non-Néel type in which the average magnetic moment vanishes at every site.¹ Even though the classical ground state is highly degenerated, small fluctuations (quantum or thermal) may induce what has been called "order from disorder"³ selecting configurations in which all spins are coplanar (spin-nematic order).^{4,5}

The simplest experimental realization of these locally frustrated geometric structures are triangles and tetrahedra. In particular the so-called *kagomé* lattice is made up of a network of corner-sharing triangles.⁶ The intrinsic frustration in combining antiferromagnetic interactions and a network of corner-sharing triangles may be easily appreciated by considering three spins in a single triangle, arranging two spins into an up-down pair implies that, no matter what the third spin is up or down, one of the two interactions is frustrated.

The ground-state properties of these geometrically frustrated systems have arisen great interest both theoretical and experimental, due to its very peculiar magnetic behavior. While some theoretical studies show that the classical Heisenberg antiferromagnet on a *kagomé* lattice is an example of a spin-nematic order,⁷ some others indicate that the ground state of the spin- $\frac{1}{2}$ quantum antiferromagnet does not possess magnetic order.^{8,9} The role played by defects has also been taken into consideration

and very recent studies show that site disorder induces noncoplanar states that compete with the thermal selection of coplanar states,¹⁰ nevertheless this disorder does not include conventional spin-glass behavior.

Among the compounds that exhibit these geometrical frustrated units the most widely studied by far are pyrochlores¹¹ (in which metal sublattices form an infinite three-dimensional network of corner-sharing tetrahedra) and the $\text{SrCr}_8\text{Ga}_4\text{O}_{19}$ compound¹² (where antiferromagnetically coupled Cr atoms are arranged in a *kagomé* lattice).

Spin-glass-like behavior has been reported for $\text{SrCr}_{8-x}\text{Ga}_{4+x}\text{O}_{19}$ compound together with an unusually low-temperature specific heat varying as T^2 instead of the typical linear T dependence of the spin glasses.¹³ It has been suggested that this T^2 form might arise from finite-size antiferromagnetic regions and that blockage might occur between the regions, allowing different physical origins, from the spin-glass freezing, for the magnetic and thermal behavior of the system.¹³ On the other hand, the effect of dilution has also been addressed^{13,14} showing that the magnetic frustration, $\theta/T_f \approx 135 \pm 5$ is independent of the degree of dilution, thus making evident the intrinsic structural origin of the magnetic frustration.

Low-temperature neutron powder diffraction¹⁵ shows the absence of long-range ordering with static correlation length that does not exceed 7 ± 2 Å and fluctuations that account for more than 75% of the free-ion moment even at $T \approx 1.5$ K, which would imply a spin-liquid ground state. However, the presence of hysteresis in the dc susceptibility^{13,14} probably excludes this scenario.

In this work we present a detailed study of the dc and

ac magnetic susceptibility of the $\text{SrCr}_8\text{Ga}_4\text{O}_{19}$ compound in order to gain a deeper insight on the nature of the magnetic transition that takes place at T_f and whether or not the system is in a conventional spin-glass state below this temperature. In addition, since the only effect of the dilution with nonmagnetic species seems to be a decrease of the freezing temperature,^{13,14} we have also studied the magnetic behavior of the system $\text{SrCr}_8\text{Ga}_{4-x}\text{Fe}_x\text{O}_{19}$ to observe what is the effect of the addition of a different magnetic moment in the magnetic frustration. We have limited our study to $x < 2$, since for this Fe concentration reentrant behavior starts to appear.¹⁶

EXPERIMENT AND RESULTS

Details about the preparation of the samples may be found elsewhere.^{14,17} dc magnetic measurements were performed by using a superconducting quantum interference device (SQUID) magnetometer in the temperature range from 1.6 to 340 K, and a Faraday balance from room temperature to 1000 K. ac magnetic susceptibility data were measured in the temperature range from 2.5 to 300 K in a Lake Shore susceptometer, where temperatures lower than 4.2 K were reached by pumping over the He bath.

Regarding to the structure of the $\text{SrCr}_8\text{Ga}_4\text{O}_{19}$ compound the most important feature is that Cr^{3+} ions do only enter in the three different octahedral sites, namely $2a$, $12k$, and $4f_{\text{VI}}$, with an almost random distribution between them ($2a$ sites are occupied with slight preference).¹⁴ In the case of the Fe-doped compound, Fe atoms substitute Ga atoms randomly. The magnetic sublattice is made up of a sequence of c -stacked two-dimensional kagomé layers ($12k$ sites). $12k$ layers are connected between them through the more diluted $2a$ and $4f_{\text{VI}}$ layers, the latter acting as bottleneck, since there are two $4f$ layers between two consecutive $12k$ layers. This stacking mimics a kagomé lattice along the c axis and leads, in fact, to a kagomé block structure made of five stacked layers ($4f_{\text{VI}}-12k-2a-12k-4f_{\text{VI}}$).

In Fig. 1 we show the reciprocal of the dc magnetic susceptibility for the two samples containing Fe atoms. A Curie-Weiss law is followed in the high-temperature region, as in the case of the sample with $x=0$.¹⁴ The values obtained for the Curie temperature Θ , and the effective magnetic moment are summarized in Table I. The values of the extrapolated Curie temperature range from -537 to -767 , making evident the existence of strong antiferromagnetic interactions in the three samples. Nevertheless, it should be pointed out that the degree of magnetic frustration, measured by the ratio $|\Theta/T_f|$, clearly decreases increasing the Fe content, going from 138 for $x=0$ to 30 for $x=1.5$. This result is in strong contrast with what is observed when doping with a nonmagnetic atom (Ga). As it has been stated previously^{13,14} changing drastically the Ga content does not affect the magnetic frustration of the system, on the contrary the addition of a small quantity of a new magnetic species (Fe) produces a strong decrease of the magnetic frustration. At the same time a strong increase of the freezing temperature T_f is also observed.

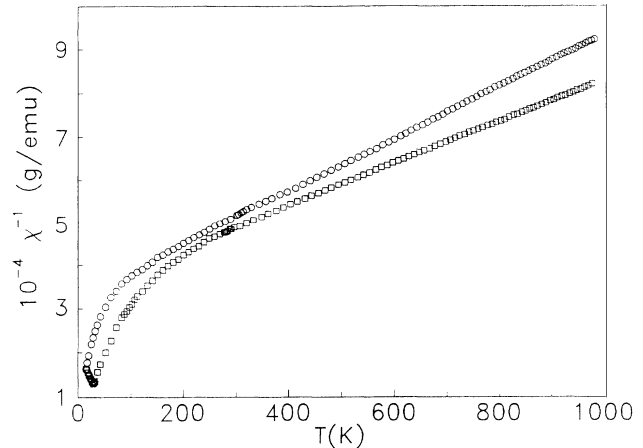


FIG. 1. Reciprocal of the dc magnetic susceptibility showing the Curie-Weiss behavior in the high-temperature range for the samples $x=0.5$ (\circ) and $x=1.5$ (\square).

Once we have made a general picture of the magnetic behavior of our samples let us focalize our attention in the main aim of this work, that is, to study the nature of the freezing phenomenon that takes place at T_f . To determine the nature of the freezing phenomenon at T_f we have studied the dependence of field-cooled (FC) magnetic susceptibility χ , as a function of both temperature and applied magnetic field from which we derive the static critical behavior. In Fig. 2 we depicted dc susceptibility curves from 3 to 15 K with the applied field varying from 20 Oe to 50 kOe; it can be observed from the figure that as a result of the nonlinear effects, the peak associated with the freezing phenomena broadens and becomes rounded as the field increases. However, the nonlinear contribution to the magnetic susceptibility becomes more evident in Fig. 3, where susceptibility data are depicted as a function of the applied field, a substantial increase of the nonlinear part of the susceptibility is observed as the freezing temperature is approached from above.

To study the nature of the transition that takes place at T_f , we have analyzed the nonlinear part of the magnetic susceptibility by developing the magnetization above T_f in terms of the odd powers of the field,¹⁸

$$M = \chi_0 H - b_3 (\chi_0 H)^3 + b_5 (\chi_0 H)^5 - \dots \quad (1)$$

being χ_0 the linear susceptibility, while the rest of the coefficients stand for the nonlinear contribution. The least-squares fit of the isothermal magnetization curves obtained from the field cooled data to Eq. (1) allows the

TABLE I. Values of the effective magnetic moment, extrapolated Curie-Weiss temperature, freezing temperature, and magnetic frustration parameter as a function of the Fe atoms concentration.

X	μ (μ_B/FU)	Θ (K)	T_f	$ \Theta/T_f $
0	3.9(1)	-537(5)	3.9	138
0.5	4.2(1)	-565(5)	9.0	62.7
1.5	4.4(1)	-767(5)	25	30.1

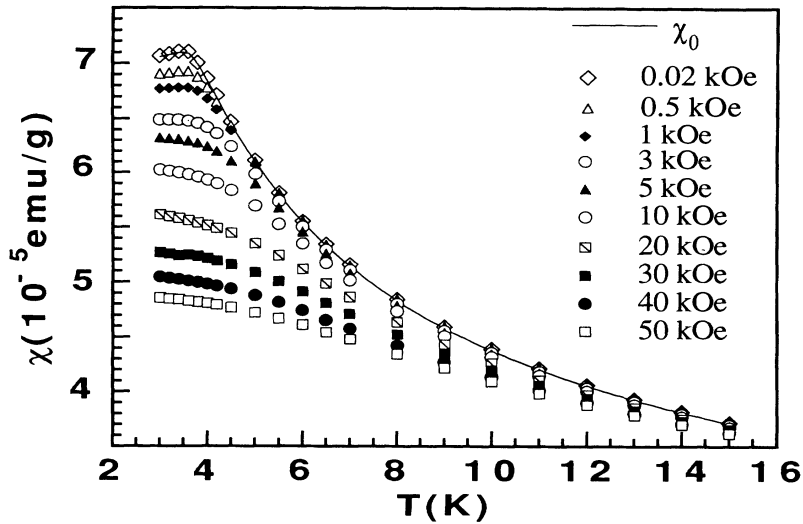


FIG. 2. Magnetic susceptibility obtained after a field-cooling process as a function of the external applied field for the sample with $x=0$. Solid line corresponds to the linear susceptibility χ_0 , obtained by fitting the experimental data to Eq. (1).

determination of the temperature dependence of χ_0 , b_3 , and b_5 .

The temperature variation of the b_3 coefficient is shown in Fig. 4; b_5 coefficient is omitted due to its very broad error band. A slight increase of the b_3 coefficient as T_f is approached from above is observed. Nevertheless, this increase is very small when compared with that observed for a typical spin glass (three orders of magnitude^{18,19}) and that is usually taken as a proof of the existence of a true spin-glass transition at T_f .¹⁸

The most relevant test of the critical behavior of a spin-glass system is obtained by measuring and analyzing the nonlinear part of the magnetic susceptibility defined by the equation

$$\chi_{nl}(H, T) = \chi_0(T) - \frac{M(H, T)}{H}, \quad (2)$$

where χ_0 is the linear susceptibility obtained through the fitting of FC experimental data to Eq. (1). In the case of a spin-glass transition a scaling behavior according to the single-parameter relation given by Eq. (3) is expected:²⁰

$$\chi_{nl}(H, T) \propto H^{2/\delta} f\left(\frac{\varepsilon}{H^{2/\phi}}\right), \quad (3)$$

where $\varepsilon = (T - T_c)/T_c$, δ and ϕ are the critical exponents that characterize the spin-glass transition, T_c is the critical temperature at which the phase transitions occurs, and $f(x)$ is an arbitrary scaling function with the following asymptotic behavior:

$$\begin{aligned} f(x) &= \text{const}, & x \rightarrow 0, \\ f(x) &= x^{-\gamma}, & x \rightarrow \infty. \end{aligned} \quad (4)$$

The critical exponent δ may be determined making use of the above asymptotic relations by the following equation:

$$\chi_{nl}(H, T_c) \propto H^{2/\delta} \quad (5)$$

that represent the asymptotic behavior of the critical isothermal as x approaches 0. In the inset of Fig. 5 we show the log-log plot of χ_{nl} as a function of H , from which, by using Eq. (5), a δ value of 5 ± 0.3 have been obtained from the slope of the linear regime. The data points for this

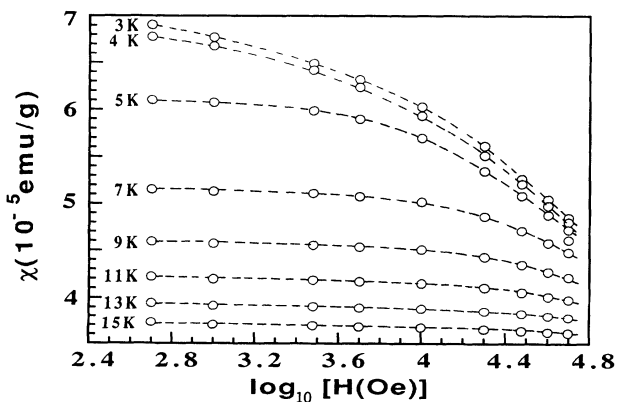


FIG. 3. Field-cooled magnetic susceptibility at selected temperatures as a function of the logarithm of the applied magnetic field.

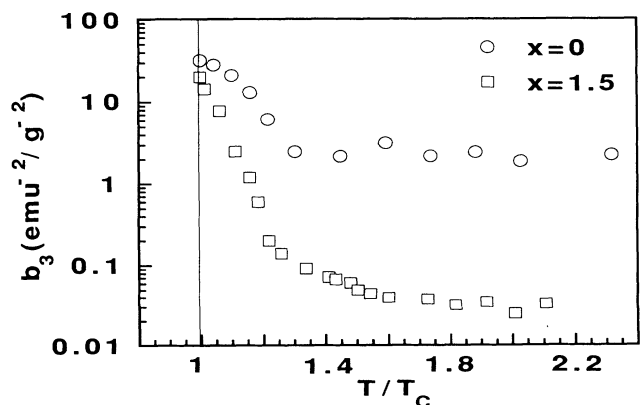


FIG. 4. Plot of the b_3 coefficient of the series expansion of the magnetization in odd powers of $(\chi_0 H)$ as a function of temperature for $\text{SrCr}_8\text{Ga}_{4-x}\text{Fe}_x\text{O}_{19}$ compound.

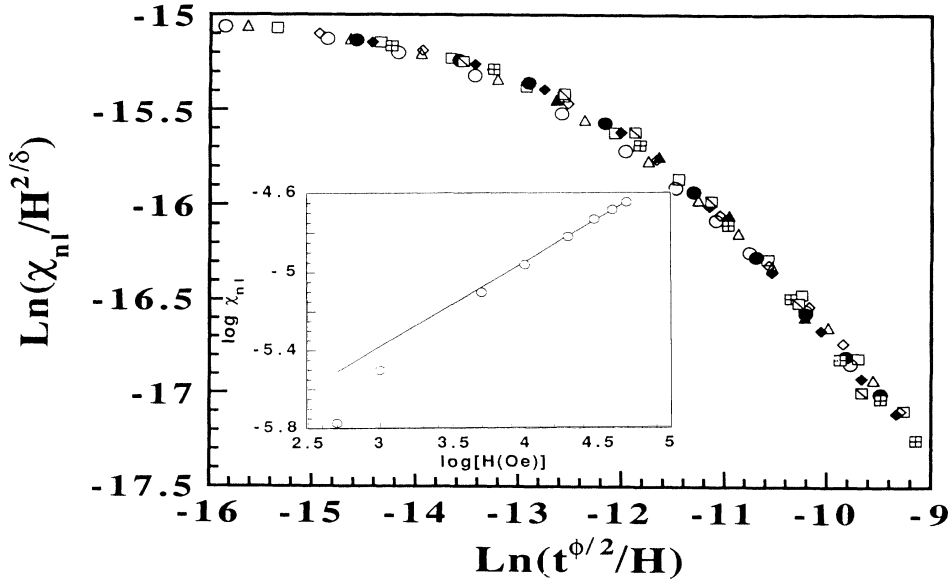


FIG. 5. Scaling plot of the nonlinear part of the susceptibility, χ_{nl} , for the $\text{SrCr}_8\text{Ga}_4\text{O}_{19}$ compound. (\circ) 50 kOe, (\triangle) 40 kOe, (\square) 30 kOe, (\diamond) 20 kOe, (\bullet) 14 kOe, (\blacklozenge) 12 kOe, (\boxplus) 10 kOe, (\boxtimes) 5 kOe, (\blacktriangle) 2 kOe. Inset: Determination of the δ value from the slope of the log-log plot of χ_{nl} as a function of H . Data at $T=3.4$ K have been used.

plot have been taken at $T=3.4$ K that corresponds to the nearest measured temperature to that at which the b_3 coefficient shows its maximum. Then we have used Eq. (3) to scale our FC data, in the temperature range $1.1T_c < T < 2T_c$, varying the values of T_c and ϕ in order to get the best data collapsing. The result is depicted in Fig. 5 and corresponds to the following set of critical exponents $\delta \approx 5 \pm 0.4$, $\phi \approx 4.4 \pm 0.5$, and a critical temperature $T_c \approx 3.45 \pm 0.1$.

The reliability of the scaling behavior and the set of critical exponents can be checked by studying the asymptotic behavior of the scaling functions given by Eq. (4). In the limit of x large with constant magnetic field (at small fields or for large values of the reduced temperature, ϵ), an asymptotic behavior of the form $x^{-\gamma}$ has to be observed, where γ is the susceptibility exponent that is related to δ and ϕ exponents through the following hyperscaling relation:²¹

$$\gamma = \phi(1 - 1/\delta). \quad (6)$$

In our case, the asymptotic slope that we obtain from the scaling plot (Fig. 5) is $-2\gamma/\phi \approx 0.68 \pm 0.1$ given a value of $\gamma \approx 1.5 \pm 0.3$ that is two times smaller than the corresponding value obtained through the hyperscaling relation expressed in Eq. (6). Even though an asymptotic constant value is observed in the limit $x \rightarrow 0$, the fact that the scaling relation given by Eq. (6) is not fulfilled with the value obtained for γ from the asymptotic slope indicates that the scaling plot we have obtained is just a mathematical relation, but it lacks of physical meaning.²¹ This fact together with the nondivergence of the b_3 and b_5 coefficients of Eq. (1) as T_f is approached from above indicates that the transition observed T_f does not correspond to the transition at a conventional spin-glass state, i.e., that the low-temperature state of the $\text{SrCr}_8\text{Ga}_4\text{O}_{19}$ is not a conventional spin glass, as its low-temperature specific heat of the T^2 form¹³ and some very recent theoretical studies¹⁰ indicate.

In order to get a more complete comprehension of the nature of the low-temperature magnetic state of the

$\text{SrCr}_8\text{Ga}_4\text{O}_{19}$ compound we have also studied its dynamical critical properties by measuring the real, χ' , and imaginary, χ'' , parts of the ac magnetic susceptibility as a function of the frequency of the ac field. In-phase magnetic susceptibility shows a peak that defines the freezing temperature, $T_f(\omega)$, that has a smooth dependence on frequency of measurement (see Fig. 6). Taking the temperature corresponding to the cusp of χ' , $T_f(\omega)$, as the onset of strong irreversibility of each measuring time $t = 1/\omega$ (being ω the frequency of the ac magnetic field) and studying its dependence on the ac field frequency the dynamical properties of the transition may be checked. There are basically two different interpretations of the freezing phenomenon: One is the cluster model, in which the system is considered as a set of superparamagnetic clusters with each cluster having a probability to overcome the anisotropy energy barrier E , following an Arrhenius or Vogel-Fulcher law.²² The other model assumes the existence of a true equilibrium phase transition, in which case the divergence of the relaxation time τ as the critical temperature is approached from above is given by:²³

$$\tau \propto \left[\frac{T_f(\omega)}{T_c} - 1 \right]^{-z_\nu}, \quad (7)$$

where ν is the critical exponent for the correlation length ξ , z is the dynamic exponent relating ξ and τ , and T_c is the phase-transition temperature. In the framework of this second model we have studied the dynamic scaling of the quantity

$$\Delta\chi' = [\chi_0(T) - \chi'(T, \omega)] / \chi_0(T), \quad (8)$$

where $\chi_0(T) = \chi'(0, T)$ is the equilibrium susceptibility that can be assumed to be equal to the linear susceptibility deduced from Eq. (1). In Fig. 6 the real part of the ac magnetic susceptibility $\chi'(T, \omega)$ is depicted for different frequencies together with the linear susceptibility $\chi_0(T)$. The above assumption that $\chi_0(T) = \chi'(0, T)$ is fully confirmed in this picture, since, as temperature increases,

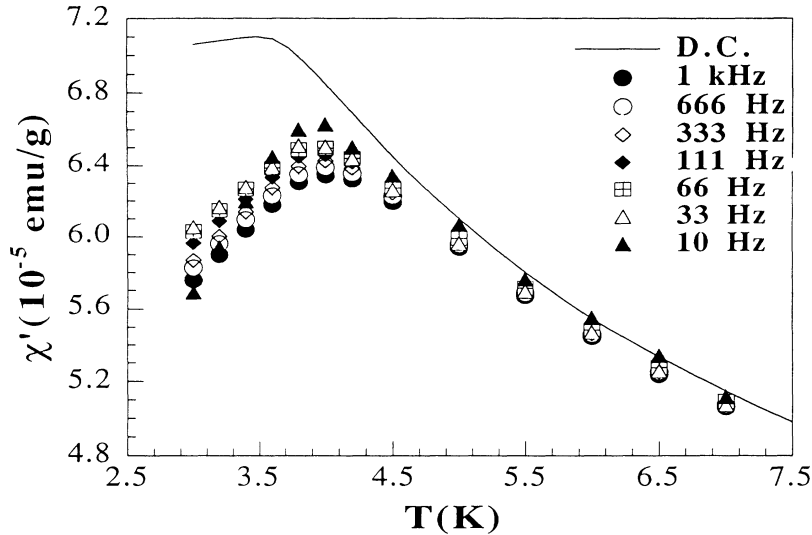


FIG. 6. Thermal dependence of the real part of the ac susceptibility χ' as a function of the frequency of the ac field for $\text{SrCr}_8\text{Ga}_4\text{O}_{19}$ sample. The solid line represents the equilibrium susceptibility obtained by fitting the dc FC data to Eq. (1).

the asymptotic behavior of $\chi'(\omega, T)$ perfectly matches the $\chi_0(T)$ curve (solid line).

It follows from Eq. (7) and (8) that $\Delta\chi'(\omega, T)$ data should assume, as $T \rightarrow T_c$ and $\omega \rightarrow 0$, the following scaling form:

$$\Delta\chi'(\omega, T) \approx (T/T_c - 1)^\beta F[\omega(T/T_c - 1)^{-z\nu}], \quad (9)$$

where β is the exponent of the order parameter and $F(x)$ a general scaling function. In Fig. 7 we depicted the results obtained by using the power law scaling given by (9) in the temperature range $T_c < T < 1.5T_c$, as in other insulator systems.²⁴ The best collapsing of the data points in a single curve is obtained with the following set of critical exponents: $z\nu \approx 9 \pm 0.3$, $\beta \approx 0.6 \pm 0.1$, and $T_c \approx 3.5 \pm 0.1$. Even though the values of the dynamic critical exponents are similar to other previously published in different spin-glass systems²⁵ and numerical simulations of three-dimensional spin glasses with short-range interactions,²⁶ the poor quality of the fitting is evident as well as the fact that the asymptotic behavior is not observed. It is also

worth mentioning that the value of the exponent $\beta \approx 0.6$, obtained from the scaling plot does not obey at all the hyperscaling relation $\beta = \phi/\delta \approx 0.9$ being ϕ and δ the critical exponents deduced from the analysis of the nonlinear part of the dc susceptibility. This fact leads us to conclude that, as in the case of the nonlinear part of the dc susceptibility, the scaling fit is merely mathematics.²¹ Then, the existence of a true phase transition to a spin-glass state at T_c seems to be also precluded from the point of view of the dynamical behavior of the system.

Since the existence of a conventional spin-glass state below T_f in the $\text{SrCr}_8\text{Ga}_4\text{O}_{19}$ compound seems to be in conflict with its statistical and dynamical behavior, it could shed some light on the magnetic state to substitute some amount of Ga by another element carrying a magnetic moment, such as Fe. As we have commented above, increasing the degree of dilution of the Cr atoms, by substituting Cr by Ga, only produces a shift of the freezing temperature, but does not affect the magnetic frustration.^{13,14} On the other hand the addition of Fe atoms produces a strong decreases of the magnetic frus-

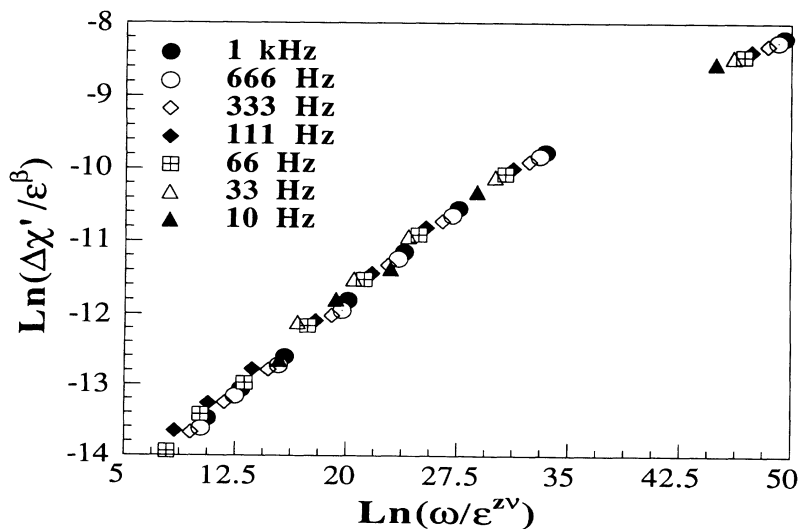


FIG. 7. Power-law scaling of $\Delta\chi'(\omega, T)$ data according to Eq. (9) for the $\text{SrCr}_8\text{Ga}_4\text{O}_{19}$ sample. Data from $T = 3.6$ to 6 K have been used.

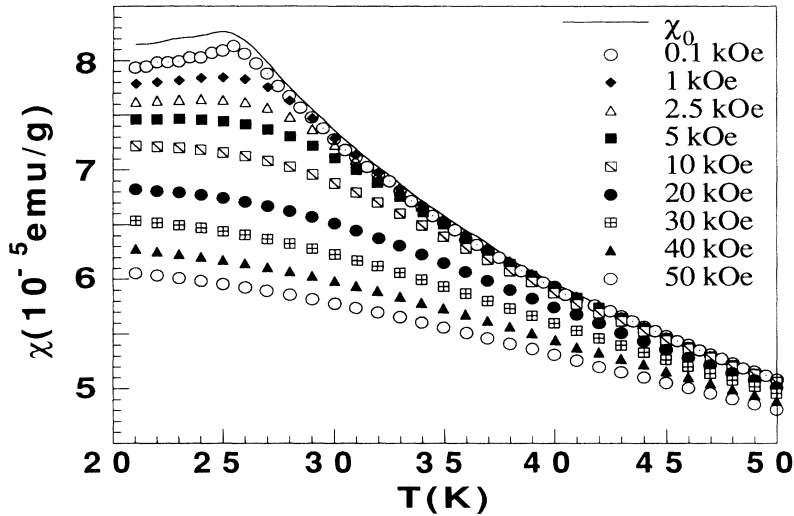


FIG. 8. Magnetic susceptibility measured after a field-cooling process as a function of the external applied field for the sample with $x=1.5$. The solid line corresponds to the linear susceptibility χ_0 , obtained by fitting the experimental data to Eq. (1).

tration as well as an increase of the freezing temperature.

In order to determine whether or not these changes also imply a change in the magnetic state below T_f we have analyzed both dc and magnetic susceptibility in the system $\text{SrCr}_8\text{Ga}_{4-x}\text{Fe}_x\text{O}_{19}$ ($x=0.5, 1.5$). In the case of the sample having $x=0.5$ we observe both an increase of the freezing temperature and a decrease of the magnetic frustration (see Table I). Nevertheless, the study of the nonlinear susceptibility makes evident that only small changes, if any, have been produced in the nature of the magnetic state below T_f , idea that is also corroborated by the observed dynamic behavior. Both static and dynamic scaling show very similar features and results to that observed in the $\text{SrCr}_8\text{Ga}_4\text{O}_{19}$ pure compound.

On the other hand, when the Fe content is further increased ($x=1.5$ sample) things start to change in a notorious way. In Fig. 8 we show the susceptibility curves from 100 Oe to 50 kOe as a function of temperature, that we have used to study the static critical behavior following the same procedure described in the case of pure

$\text{SrCr}_8\text{Ga}_4\text{O}_{19}$ ($x=0$ sample). In the inset of Fig. 9 the log-log plot of χ_{nl} as a function of H is depicted, from this data, by using Eq. (5), we have deduced a value of $\delta \approx 4.5 \pm 0.2$ from the slope of the linear regime. Note that in this case the linear regime holds for a very wide range of field sin contrast with the case of the $x=0$ sample that exhibits linear regime for very high fields only ($H > 10$ kOe). Using this value for δ we have scaled the FC data in Fig. 8 according to Eq. (3) varying T_c and ϕ in order to get the best data collapsing in a single curve. The best result obtained is depicted in Fig. 9 and corresponds to the following set of critical exponents: $\delta \approx 4.5 \pm 0.3$, $\phi \approx 4.5 \pm 0.4$, and a critical temperature $T \approx 24.9 \pm 0.1$ K.

The asymptotic slope obtained from the scaling plot in Fig. 9 is $-2\gamma/\phi \approx -1.5 \pm 0.1$, which gives a value of $\gamma \approx 3.4 \pm 0.4$ that is very good agreement with the corresponding value obtained through the hyperscaling relation given by Eq. (6) ($\gamma \approx 3.5 \pm 0.3$) at the same time, the asymptotic constant value is also observed in the limit $x \rightarrow 0$. Regarding the set of critical exponents we have

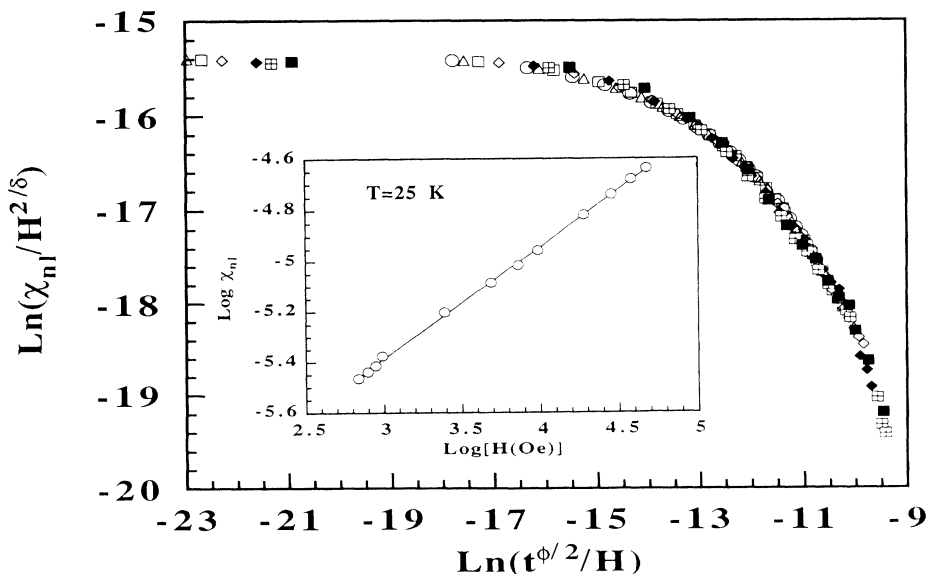


FIG. 9. Scaling plot of the nonlinear part of the susceptibility χ_{nl} for the $\text{SrCr}_8\text{Ga}_{2.5}\text{Fe}_{1.5}\text{O}_{19}$ samples: (\circ) 50 kOe, (\triangle) 40 kOe, (\square) 30 kOe, (\diamond) 20 kOe, (\blacklozenge) 10 kOe, (\boxtimes) 7.5 kOe, (\blacksquare) 5 kOe. Inset: Determination of the δ value from the slope of the log-log plot of χ_{nl} as a function of H . Data at $T=25$ K have been used.

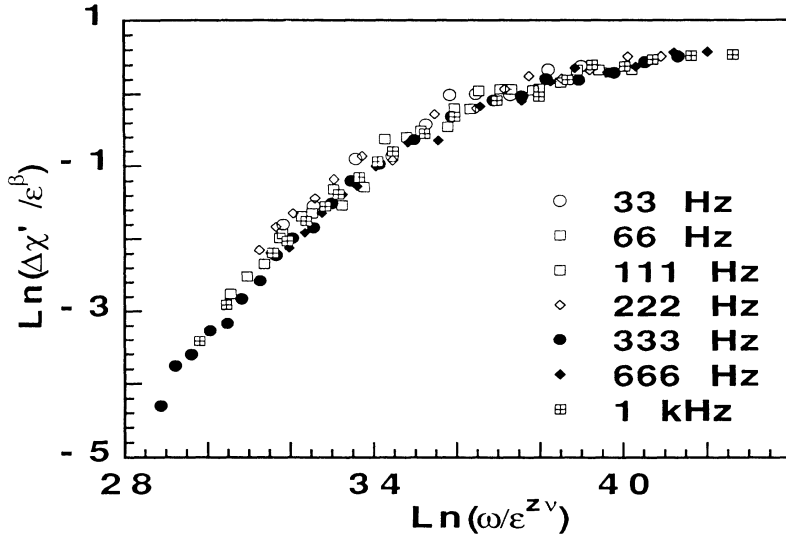


FIG. 10. Power-law scaling of $\Delta\chi'(\omega, T)$ data according to Eq. (9) for the $\text{SrCr}_8\text{Ga}_{2.5}\text{Fe}_{1.5}\text{O}_{19}$ sample. Data from $T = 25.2$ to 28 K have been used.

used, it is worth noting that they are in very good agreement with those reported for insulating-type spin glasses, for which typical values are $\delta \approx 4 \pm 0.5$ and $\phi \approx 3.5 \pm 0.5$,^{27,28} but different from those reported, for example, in $\text{BaCo}_6\text{Ti}_6\text{O}_{19}$,¹⁹ which has a very similar structure, or $\text{Fe}_{0.5}\text{Mn}_{0.5}\text{TiO}_3$.²⁹ Then, from the point of view of the scaling theory it seems possible to conclude that in the case of the $\text{SrCr}_8\text{Ga}_{2.5}\text{Fe}_{1.5}\text{O}_{19}$ sample a conventional spin-glass phase transition takes place at T_c . Nevertheless, we should remark here that b_3 and b_5 coefficients of Eq. (1), even though they show a considerable increase when compared with those of the pure compound, do not diverge as T_f is approached from above (see Fig. 4).

We have also checked the dynamic properties of the system by analyzing the scaling behavior according to Eq. (9). The best data collapsing of the experimental points to a single curve (see Fig. 10) is obtained with the following set of critical exponents: $z\nu \approx 10 \pm 0.5$, $\beta \approx 1 \pm 0.2$, and $T_c \approx 24.9 \pm 0.1$ K. It is worth mentioning here that, even the quality of the scaling plot (see Fig. 10) is similar to that of the pure compound (Fig. 7), in this case the asymptotic behavior is properly observed and the value of the β exponent also complies with the hyperscaling relation $\beta = \phi/\delta$ (using the values of ϕ and δ deduced from the static analysis), relation that is not observed for the pure compound.

The set of critical exponents obtained from the scaling analysis compare well with those previously published for semimagnetic semiconductors,²⁵ $\text{BaCo}_6\text{Ti}_6\text{O}_{19}$,¹⁹ and also with results of numerical simulation in the case of three-dimensional spin glasses with short-range interactions.²⁶ Then, dynamic scaling analysis also gives further clues to the existence of a true equilibrium phase transition at T_c to a low-temperature conventional spin-glass phase.

CONCLUSIONS

We have carefully analyzed both dc and ac magnetic susceptibility in the highly frustrated $\text{SrCr}_8\text{Ga}_4\text{O}_{19}$ compound to study the properties of its low-temperature magnetic state and to determine whether or not a conven-

tional spin glass state exists below T_f . The high magnetic frustration in this compound arises from the Cr^{3+} ions, interacting antiferromagnetically, arranged in a corner-sharing triangular lattice (kagomé lattice) in the 12k planes.

Even though the scaling of the nonlinear part of the dc susceptibility χ_{nl} appears to be of good quality and the critical exponents are similar to others reported for spin glasses, it turns out to be a mathematical fit lacking of its physical meaning, since the value of the γ exponent obtained from the asymptotic slope in the limit of $x \rightarrow \infty$ does not comply with the hyperscaling relation given by Eq. (6).²¹ The different asymptotic slope observed in Figs. 5 and 9 has nothing to do with the different scale used in each figure, and reflects the different intrinsic behavior of each sample. Furthermore, b_3 and b_5 coefficients of Eq. (1) show only a small increase approaching T_f from above, while the divergence of both coefficients should occur in the case of a true spin-glass transition.¹⁸ These facts seem to indicate that the magnetic state below T_f of the $\text{SrCr}_8\text{Ga}_4\text{O}_{19}$ compound does not correspond to a conventional spin-glass state. Similarly, the analysis of the dynamical critical behavior also points to a nonconventional spin-glass state below T_f .

As some number of Ga atoms are substituted by Fe ($\text{SrCr}_8\text{Ga}_{4-x}\text{Fe}_x\text{O}_{19}$), which carry a magnetic moment that may help to increase magnetic interaction between different 12k planes, a smooth change of the magnetic behavior towards that of a conventional spin glass is observed. In the case of the sample with $x = 1.5$ we obtain a good scaling of the nonlinear part of the dc magnetic susceptibility with critical exponents that are in good agreement with others previously reported for typical spin-glass systems. Furthermore, in this case both asymptotic behavior and hyperscaling relations between the different critical exponents are observed. The analysis of the dynamical behavior of this sample also shows a proper scaling with exponents that compare well with those previously reported and complies with the hyperscaling relation $\beta = \phi/\delta$ using the values of ϕ and δ deduced from the static analysis. Then, both the dynam-

ic and the static scaling analysis seem to indicate that, in the case of the $\text{SrCr}_8\text{Ga}_{2.5}\text{Fe}_{1.5}\text{O}_{19}$ sample, a true transition to a conventional spin glass state takes place at T_c .

In order to understand the effect of the introduction of Fe atoms, that randomly substitute Ga atoms, in the structure we shall bear in mind the hierarchy or the magnetic interactions. It turns out from Ref. 30 that

$$J_{12k-4f_{VI}} > J_{4f_{VI}-4f_{VI}} > J_{12k-12k} > J_{12k-2a},$$

what this implies is that as Fe atoms do substitute Ga atoms in the structure, two effects that greatly affect the intrinsic magnetic frustration of the kagomé lattice ($12k$ sites) takes place. One is the substantial increase of the probability to find a path for the magnetic interaction between two kagomé planes across the bottlenecklike structure made up of two stacked $4f_{VI}$ planes. Then the ap-

pearance of three-dimensional short-range magnetic correlations may be greatly favored. The other one is also the increase of the probability to find a magnetic atom as a nearest neighbor in the $4f_{VI}$ layer for a Cr atom located in a $12k$ site. Since $J_{12k-4f_{VI}}$ interactions are very much stronger than $J_{12k-12k}$ interactions the presence of Fe atoms in $4f_{VI}$ sites will impose a “preferential direction” for the orientation of the spins removing somehow the “degenerate disorder” imposed by the intrinsic geometrical frustration of the kagomé lattice. These facts are reflected in a progressive change from the low-temperature frozen state with “degenerate disorder” that is observed in the case of the $\text{SrCr}_8\text{Ga}_4\text{O}_{19}$ pure compound to the conventional spin-glass ordering that is observed in the case of $\text{SrCr}_8\text{Ga}_{2.5}\text{Fe}_{1.5}\text{O}_{19}$ sample.

- ¹P. Fazekas and P. W. Anderson, *Philos. Mag.* **30**, 423 (1974).
²P. Chandra and B. Doucot, *Phys. Rev. B* **38**, 9335 (1988).
³J. Villain, R. Bidaux, J. P. Carton, and R. Conte, *J. Phys. (Paris)* **41**, 1263 (1980); A. Chubukov, *Phys. Rev. Lett.* **69**, 832 (1992).
⁴P. Chandra and P. Coleman, *Phys. Rev. Lett.* **66**, 100 (1991).
⁵P. Chandra, P. Coleman, and A. I. Larkin, *J. Phys. Condens. Matter* **2**, 7933 (1990); P. Chandra, P. Coleman, and I. Ritchey, *J. Appl. Phys.* **69**, 4974 (1991).
⁶I. Syozi, in *Phase Transitions and Critical Phenomena*, edited by C. Domb and M. S. Green (Academic, New York, 1972), p. 269.
⁷J. T. Chalker, P. C. W. Holdsworth, and E. F. Shender, *Phys. Rev. Lett.* **68**, 855 (1992); A. B. Harris, C. Kallin, and A. J. Berlinsky, *Phys. Rev. B* **45**, 2899 (1992).
⁸J. T. Chalker and J. F. G. Eastmond, *Phys. Rev. B* **46**, 14 201 (1992).
⁹P. W. Leung and Veit Elser, *Phys. Rev. B* **47**, 5459 (1993).
¹⁰E. F. Shender, V. B. Cherepanov, P. C. W. Holdsworth, and A. J. Berlinsky (unpublished).
¹¹B. D. Gaulin, J. N. Reimers, T. E. Mason, J. E. Greedan, and Z. Tun, *Phys. Rev. Lett.* **69**, 3244 (1992); J. N. Reimers, J. E. Greedan, C. V. Stager, and M. Bjorgvinnsen, *Phys. Rev. B* **43**, 5692 (1991); J. E. Greedan, J. N. Reimers, C. V. Stager, and S. L. Penny, *ibid.* **43**, 5682 (1991); J. N. Reimers, J. E. Greedan, R. K. Kermer, E. Gmelin, and M. A. Subramanian, *ibid.* **43**, 3387 (1991).
¹²X. Obradors, A. Labarta, A. Isalgúe, J. Tejada, J. Rodriguez, and M. Pernet, *Solid State Commun.* **65**, 189 (1988).
¹³A. P. Ramirez, G. P. Espinosa, and A. S. Cooper, *Phys. Rev. Lett.* **64**, 2070 (1990); *Phys. Rev. B* **45**, 2505 (1992).
¹⁴B. Martínez, F. Sandiumenge, A. Rouco, A. Labarta, J. Rodríguez, M. Tovar, M. T. Causa, S. Galí, and X. Obradors, *Phys. Rev. B* **46**, 10 786 (1992); A. Rouco, F. Sandiumenge, B. Martínez, S. Galí, M. Tovar, and X. Obradors, *J. Magn. Magn. Mater.* **104-107**, 1645 (1992).
¹⁵C. Broholm, G. Aeppli, G. P. Espinosa, and A. S. Cooper, *J. Appl. Phys.* **69**, 4968 (1991); *Phys. Rev. Lett.* **65**, 3173 (1990).
¹⁶X. Obradors, A. Labarta, J. Tejada, J. L. Tholence, and M. Saint-Paul, *J. Appl. Phys.* **63**, 4091 (1988).
¹⁷X. Obradors, A. Isalgúe, A. Collomb, M. Pernet, J. Panetier, J. Rodríguez, J. Tejada, and J. C. Joubert, *IEEE Trans. Magn. MAG-20*, 1636 (1984).
¹⁸R. Omari, J. J. Prejean, and J. Souletie, *J. Phys. (Paris)* **44**, 1069 (1983).
¹⁹A. Labarta, X. Batlle, B. Martínez, and X. Obradors, *Phys. Rev. B* **46**, 8994 (1992).
²⁰B. Barbara, A. P. Malozemoff, and Y. Imry, *Phys. Rev. Lett.* **47**, 1852 (1981); A. P. Malozemof and B. Barbara, *J. Appl. Phys.* **57**, 3410 (1985).
²¹A. Gavrin, J. R. Childress, C. L. Chein, B. Martinez, and M. B. Salamon, *Phys. Rev. Lett.* **64**, 2438 (1990); A. Mauger, J. Villain, and Y. Zhou, *Phys. Rev. B* **41**, 4587 (1990).
²²L. Néel, *Ann. Geophys.* **5**, 99 (1949); J. L. Tholence, *Solid State Commun.* **35**, 113 (1980).
²³P. C. Hohenberg and B. I. Halperin, *Rev. Mod. Phys.* **49**, 435 (1977).
²⁴N. Bontemps, J. Rajchenbach, R. V. Chanberlin, and R. Orbach, *Phys. Rev. B* **30**, 6514 (1984); A. Mauger, J. Ferré, and P. Beauvillain, *ibid.* **40**, 862 (1989).
²⁵Y. Zhou, C. Rigaux, A. Mycilesky, M. Menant, and N. Bontemps, *Phys. Rev. B* **40**, 8111 (1989).
²⁶A. T. Ogielski, *Phys. Rev. B* **32**, 7384 (1985).
²⁷H. Maletta and W. Felsch, *Phys. Rev. B* **20**, 1245 (1979).
²⁸E. Vincent and J. Hammann, *J. Phys. C* **20**, 2659 (1987).
²⁹K. Gunnarsson, P. Svedlindh, P. Nordblad, L. Lundgren, H. Argua, and A. Ito, *Phys. Rev. B* **43**, 8199 (1991).
³⁰A. Isalgúe, A. Labarta, J. Tejada, and X. Obradors, *Appl. Phys. A* **39**, 221 (1986).